Bioluminescent Model for the Quantification of Photothermal Ablative Breast Cancer Therapy Mediated by Near-Infrared Nanoparticles

L. Gutwein[*], A. Singh[**], M. Hahn[**], M. Rule[*], S. Brown[**], J. Knapik[***], B. Moudgil[**], and S. Grobmyer[*]
[*]Division of Surgical Oncology, Department of Surgery, College of Medicine, [**]Particle Engineering Research Center, and [***]Department of Pathology, University of Florida

ABSTRACT

Multifunctional theranostic nanoparticles hold promise for enabling non-invasive image guided cancer therapy such as photothermal therapy. Human breast tumor models in which response to image guided therapy can quickly and non-invasively be determined are needed to facilitate translation and application of these technologies. We hypothesize that a system utilizing a murine light-reporter mammary tumor cell line and near-infrared nanoparticles (NIR-NP) can be used to quantify response to therapy and determine fate of nanoparticles following photothermal ablation.

Keywords: bioluminescence, fluorescence, photothermal ablation, live animal imaging, near-infrared nanoparticles

INTRODUCTION

Bioluminescent and fluorescent optical imaging modalities are established techniques in cancer research. Utilizing a bioluminescent light-reporter mammary tumor cell line allows dynamic real-time data quantification and temporal analysis in response to therapeutic strategies. This imaging strategy is revolutionizing cancer research and offers the potential to streamline drug discovery and development[1, 2]. NIR-NP are theranostic (the ability to diagnose and treat through one modality) nanomaterials engineered to optimally absorb and emit light in the near-infrared (NIR) region (650-900 nm). The NIR region is favored because the absorption coefficients of water and hemoglobin are at their lowest enabling deep penetration of light into tissue without harmful effects[3]. NIR-NP are efficient in optothermal energy conversion killing tumor cells in the process[4, 5]. Nanoparticle mediated photothermal therapy is actively investigated and offers a non-invasive cancer treatment[3, 4, 6-12]. In the present study, we investigate the ability of a bioluminescent murine mammary tumor model to benchmark the diagnostic imaging and therapeutic heating properties of novel NIR-NP which have the potential to revolutionize breast cancer diagnosis and treatment.

METHODS

The 4T1 murine mammary tumor cell line expressing the firefly luciferase enzyme[13] was orthotopically implanted (10^6 cells) into female BALB/c mice. For these experiments, near-infrared dye containing silica nanoparticles (40nm) were utilized. On post-implantation day 8, mice were imaged via fluorescence (710 nm excitation/820 nm emission) and bioluminescence (image obtained 10 minutes post 100 μL luciferin (15 mg/ml) intra-peritoneal injection) with the IVIS Spectrum (Caliper Life Sciences). Mice were randomly distributed to 3 groups including NIR-NP/+ablation, NIR-NP/-ablation, and control/+ablation. Mice underwent NIR-NP intratumoral injection (15 mg/mL, 20 μL) or 0.9% NaCl (20 μL). Fluorescent imaging was obtained on all mice after intratumoral injection. Mice then underwent photothermal ablative therapy (continuous wave laser, 785 nm, 500 mW, 5 minute duration, 1.5 cm source-tumor distance). Fluorescent imaging was obtained after photothermal ablation. All mice then underwent bioluminescent imaging. On post-ablation day 1, all mice underwent fluorescent/bioluminescent imaging and subsequently were sacrificed. Tumors were harvested and preserved in 10% neutral buffered formalin. Histological tumor analysis was performed in a blinded fashion and quantified as percent necrosis by a board certified pathologist. Region of interest (ROI) quantification of fluorescent and bioluminescent signals was performed at all imaging points with Living Image 3.2 software (Caliper Life Sciences).

RESULTS

Bioluminescent imaging quantification (Figure 1 a, b, c) displays a significant decrease in signal for NIR-NP/+ablation as compared to NIR-NP/-ablation and control/+ablation. This significant signal decrease remained 1 day post-ablation.

Figure 1 (a)

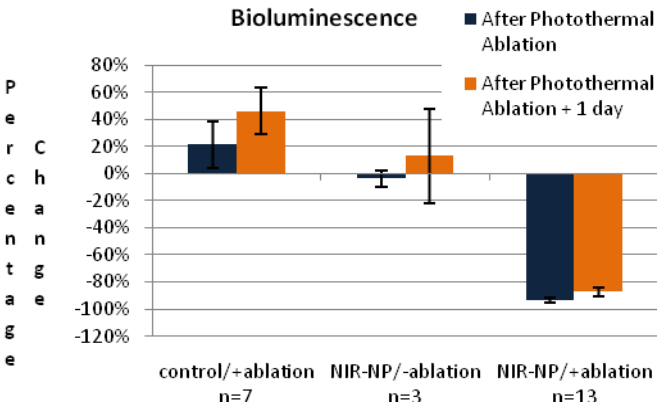

Figure 1(b) NIR-NP/+ablation (before ablation)

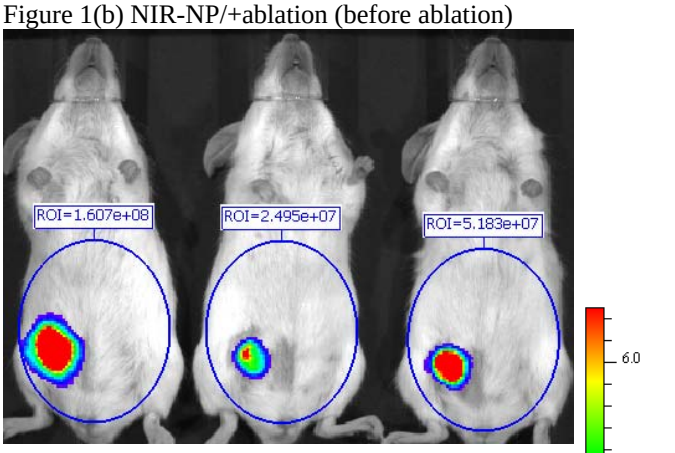

Figure 1(c) NIR-NP/+ablation (after ablation)

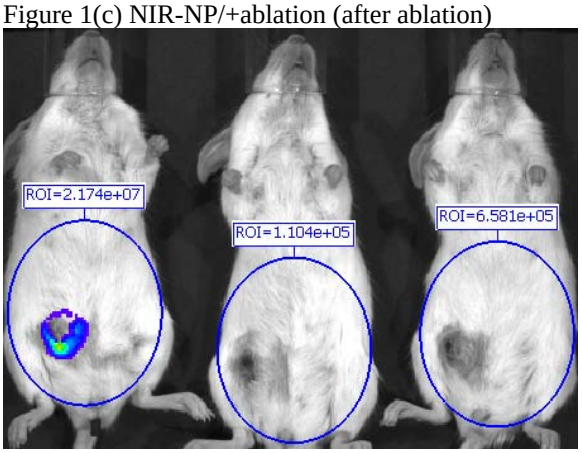

Figure 1: (a) Quantification of bioluminescent signal as a percentage change from before photothermal ablation to after photothermal ablation. (b) Bioluminescent image of NIR-NP/+ablation group before ablation and (c) after ablation. Region of interest (ROI) quantified in photons/second. *Image Acquisition Settings: excitation filter = block, emission filter = 620 nm, binning = medium, field of view = 13.2 cm, f-stop = 1, exposure = (b) 3 seconds (c) 30 seconds*

In order to explore the mechanism of the observed drop in bioluminescence following photothermal ablation of nanoparticle treated tumors (Figure 1), we analyzed the impact of intratumoral luciferin delivery and the kinetics of bioluminescence following intra-peritoneal delivery of luciferin. No change in bioluminescent signal was observed following intratumoral delivery of luciferin (10 µl, 15 mg/ml) (Data not shown). There was also no significant change in the kinetics of bioluminescence following photothermal ablation via intra-peritoneal delivery of luciferin (Data not shown).

In order to determine if the observed changes in bioluminescence correlated with cell damage, we compared necrosis in treated and control tumors 1 day following ablation (Figure 2 a, b, c). There is a significant increase in necrosis as observed by hematoxylin and eosin staining in NIR-NP/+ablation group compared to controls. This corresponds to the persistent drop in bioluminescence observed in these animals on post-ablation day 1 (Figure 1 c).

Figure 2 (a)

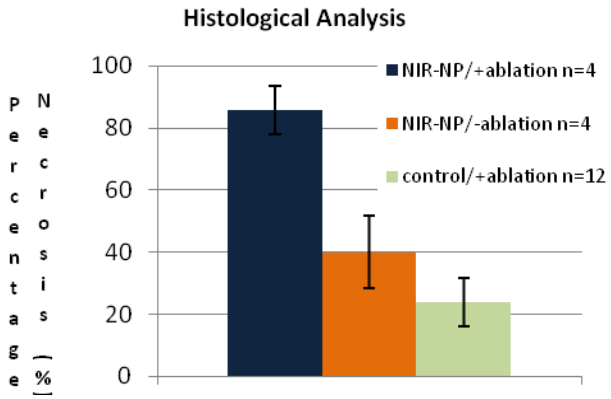

Figure 2 (b)

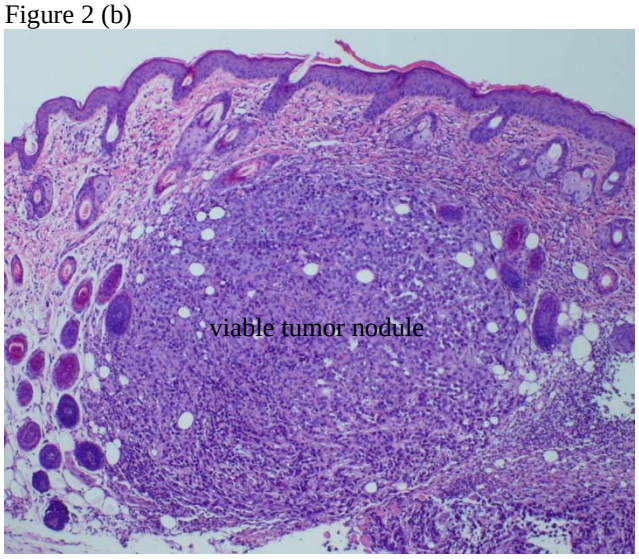

Figure 2 (c)

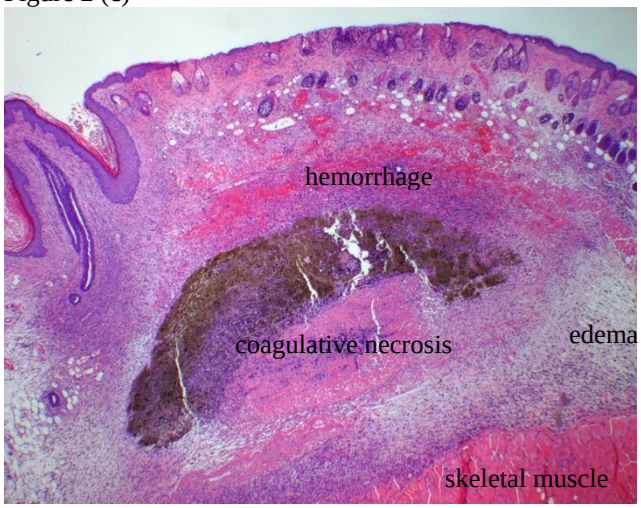

Figure 2: (a) Quantification of necrosis, (b) hematoxylin and eosin stained tumor section of control/+ablation, 4X and (c) NIR-NP/+ablation, 2X.

To assess intratumoral delivery of NIR-NP and the fate of NIR-NP following photothermal ablation, whole animal fluorescent imaging was performed. Fluorescent imaging quantification (Figure 3 a, b, c) displays a significant signal increase for NIR-NP intratumoral injection as compared to control, indicating imaging ability of NIR-NP within the tumor. On post-ablation day 1 NIR-NP signal remained within the tumors.

Figure 3 (a)

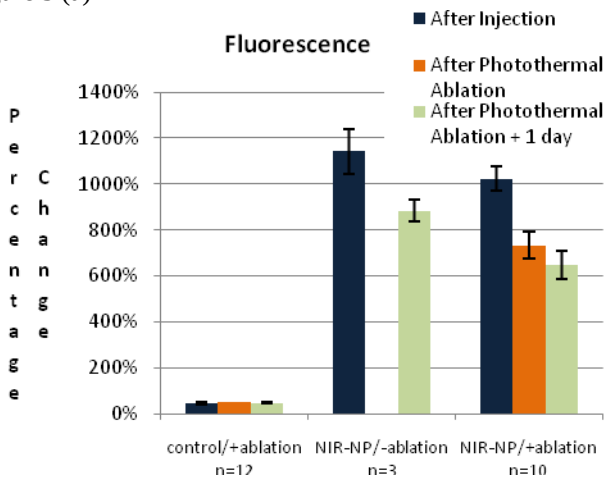

Figure 3 (b) NIR-NP/+ablation (before ablation)

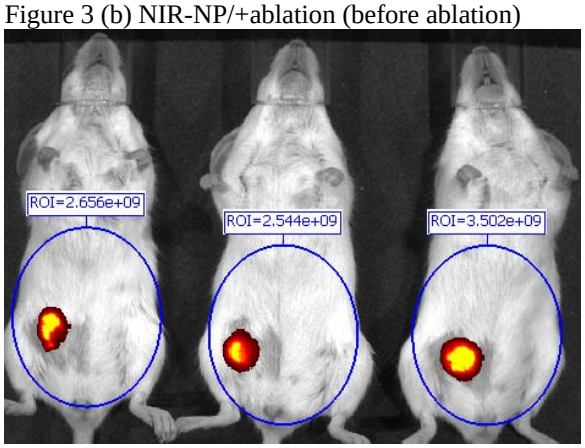

Figure 3 (c) NIR-NP/+ablation (after ablation)

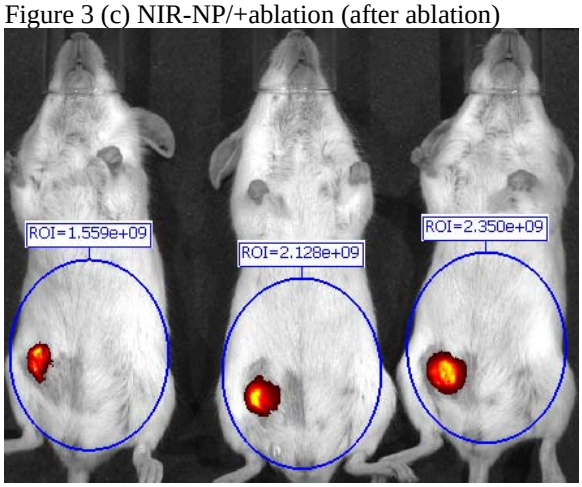

Figure 3: (a) Quantification of fluorescent signal as a percentage change from before intratumoral injection to after intratumoral injection and photothermal ablation. (b) Fluorescent image of NIR-NP/+ablation group before ablation and (c) after ablation. Region of interest (ROI) quantified in photons/second. *Image Acquisition Settings: excitation filter = 710 nm, emission filter = 820 nm, binning = small, field of view = 13.2 cm, f-stop = 2, exposure = 3 seconds*

DISCUSSION

The presently described bioluminescent murine mammary tumor model provides real-time feedback to benchmark nanoparticles as *in-vivo* phototheramal agents for cancer therapy. Importantly, this allows rapid assay of the biologic impact of photothermal agents. The drop in bioluminescence following photothermal ablation in these studies correlates with observed increases in tumor necrosis. Histological analysis in the NIR-NP/+ablation group revealed edema, coagulation, cell shrinkage, and loss of nuclear staining localized with the NIR-NP consistent with other reports[8, 12]. The observed change in bioluminescence does not correlate with changes in vascular permeability or an alteration in kinetics of the luciferin-luciferase enzymatic reaction. This model offers

an alternative to other laborious and costly measures of photothermal tumor destruction including serial tumor measurements and survival studies in mice. This bioluminescent model can also be applied to deep tumor orthotopic models in which monitoring response to photothermal therapy has historically been problematic. Intratumoral delivery of photoablative nanomaterials as demonstrated herein, may represent a therapeutically relevant approach to photothermal tumor therapy. The near-infrared dye doped nanoparticles utilized in this study allow assessment of the fate of the nanomaterials following ablation. We demonstrated that the nanoparticles remain primarily in the intratumoral position following ablation. Slight decreases in fluorescence may be due to nanoparticle degradation or extravasation from tumors following photothermal ablation. These observations on the fate of nanomaterials following photothermal ablation raise the possibility for sequential photoablative approaches to achieve complete tumor destruction and/or treatment of recurrent tumors.

CONCLUSION

The described bioluminescent model represents a novel tool for the assessment of the biologic response to photothermal therapy. It can be used to rapidly assess the response to photothermal therapy in orthotopic rodent models of human cancer. Intratumoral delivery of nanoparticles may represent a relevant approach to treatment of tumors with photothermal ablative therapy.

REFERENCES

1. Dothager, R.S., et al., *Advances in bioluminescence imaging of live animal models.* Curr Opin Biotechnol, 2009. **20**(1): p. 45-53.
2. Thorne, S.H.C.C.H., *Using in Vivo Bioluminescence Imaging to Shed Light on Cancer Biology.* Proceedings of the IEEE, 2005. **93**(4): p. 13.
3. Morton, J.G., et al., *Nanoshells for photothermal cancer therapy.* Methods Mol Biol, 2010. **624**: p. 101-17.
4. Carpin, L.B., et al., *Immunoconjugated gold nanoshell-mediated photothermal ablation of trastuzumab-resistant breast cancer cells.* Breast Cancer Res Treat, 2010.
5. Wang, C. and J. Irudayaraj, *Multifunctional magnetic-optical nanoparticle probes for simultaneous detection, separation, and thermal ablation of multiple pathogens.* Small, 2010. **6**(2): p. 283-9.
6. Bernardi, R.J., et al., *Immunonanoshells for targeted photothermal ablation in medulloblastoma and glioma: an in vitro evaluation using human cell lines.* J Neurooncol, 2008. **86**(2): p. 165-72.
7. Gobin, A.M., et al., *Near-infrared-resonant gold/gold sulfide nanoparticles as a photothermal cancer therapeutic agent.* Small, 2010. **6**(6): p. 745-52.
8. Hirsch, L.R., et al., *Nanoshell-mediated near-infrared thermal therapy of tumors under magnetic resonance guidance.* Proc Natl Acad Sci U S A, 2003. **100**(23): p. 13549-54.
9. Loo, C., et al., *Immunotargeted nanoshells for integrated cancer imaging and therapy.* Nano Lett, 2005. **5**(4): p. 709-11.
10. Lowery, A.R., et al., *Immunonanoshells for targeted photothermal ablation of tumor cells.* Int J Nanomedicine, 2006. **1**(2): p. 149-54.
11. Lu, W., et al., *Targeted photothermal ablation of murine melanomas with melanocyte-stimulating hormone analog-conjugated hollow gold nanospheres.* Clin Cancer Res, 2009. **15**(3): p. 876-86.
12. Moon, H.K., S.H. Lee, and H.C. Choi, *In vivo near-infrared mediated tumor destruction by photothermal effect of carbon nanotubes.* ACS Nano, 2009. **3**(11): p. 3707-13.
13. Tao, K., et al., *Imagable 4T1 model for the study of late stage breast cancer.* BMC Cancer, 2008. **8**: p. 228.